Analysis of aeroelastic loads and their contributions to fatigue damage

Bergami, Leonardo; Gaunaa, Mac

Published in:
Journal of Physics: Conference Series (Online)

Link to article, DOI:
10.1088/1742-6596/555/1/012007

Publication date:
2014

Document Version
Early version, also known as pre-print

Analysis of aeroelastic loads and their contributions to fatigue damage

L Bergami and M Gaunaa

Technical University of Denmark, Department of Wind Energy
Risø Campus, Roskilde - Denmark

E-mail: leob@dtu.dk

Abstract. The paper presents an analysis of the aeroelastic loads on a wind turbine in normal operation. The characteristic of the loads causing the highest fatigue damage are identified, so to provide indications to the development of active load alleviation systems for smart-rotor applications. Fatigue analysis is performed using rain-flow counting and Palmgren-Miner linear damage assumption; the contribution to life-time fatigue damage from deterministic load variations is quantified, as well as the contributions from operation at different mean wind speeds. A method is proposed to retrieve an estimation of the load frequencies yielding the highest fatigue contributions from the bending moment spectra. The results are in good agreement with rain-flow counting analysis on filtered time series, and, for the blade loads, show dominant contributions from frequencies close to the rotational one; negligible fatigue contributions are reported for loads with frequencies above 2 Hz.

1. Introduction

The size of modern utility-scaled horizontal-axis wind turbines shows a continuously increasing trend. As the rotor size increases, so do the loads that act on the turbine. Recent studies have proposed *smart-rotor* concepts, where the wind turbine actively alleviates the loads it would have to withstand; several solutions have been investigated, using either conventional pitch actuators [1, 2], or active aerodynamic devices distributed along the blade span, such as micro-tabs [3], or trailing-edge flaps [4, 5].

In most cases, the primary objective of the smart-rotor is to reduce the fatigue loads that the turbine experiences during normal production. The aim of this paper is to contribute to smart-rotor research by identifying the characteristics of the aeroelastic loads that are responsible for the largest fatigue contributions. The loads yielding the higher fatigue contributions are the ones the active alleviation system should focus on; therefore, their characteristics will provide useful indications for the design of a smart-rotor system.

The loads are characterized in terms of: stochastic and deterministic components, fatigue damage equivalent loads (DEL) contribution from rain-flow counting analysis, and spectral content; a particular focus is given to the estimation of the frequency characteristics of the loads causing the highest contribution to the fatigue damage. The four points determine the structure of the paper, and each of them is dealt with in a separate section.

The analysis builds on simulations of loads time series for the NREL 5-MW reference wind turbine [6] in its on-shore configuration. The response of the turbine is simulated using the aeroelastic code HAWC2 [7], which includes a multi-body structural model, and a BEM-based

aerodynamic model; modeling the unsteady effects of the airfoils aerodynamic forces has proved necessary to avoid biased estimations of the fatigue loads [8], hence the aerodynamic model by Hansen et al. [9] is adopted. The turbine has variable speed regulation below rated power, and collective pitch-to-feather control above rated; the standard controller by Jonkman et al. [6] is applied.

As most of the fatigue loads originate during normal operation, simulation conditions are set according to the design load case (DLC) 1.1 in the IEC standard [10]. A turbulent wind field is generated according to class IIb specifications, including the effects of tower shadow, and the terrain shear, as prescribed in the standard [10]; six turbulent series of ten minutes each are simulated for every mean wind speed.

2. Deterministic and stochastic characterization

The fatigue damage on the wind turbine structure originates from the load variations and, in a first approximation, it does not depend on the mean load level. In this study, the load variations at the blade root are classified as *deterministic*, or *stochastic*. It is chosen to define as *deterministic* the load variations that present themselves in regular cycles, where the cycle period corresponds to the period of one rotor revolution; the remaining load variations are defined as non-deterministic, or *stochastic*.

The blade root bending moment from the simulated time series are plotted as function of the blade azimuthal position, green dots in figure 1. The variation of the loads around the mean level directly relates to the fatigue damage, and is here described as three-times the loads standard deviation, red lines in figure 1. The *deterministic* contribution is assumed to be responsible for the underlying trend in the load variation, and is thus estimated as the mean load value for each azimuthal position (black line in figure 1). The remaining load variations, once the deterministic ones are filtered out, are considered *stochastic* contribution (blue lines in figure 1).

The deterministic loads are related to variations in the wind field which are constant throughout the simulated one hour series; in this case, they represent the effects of terrain shear and rotor tilt as sampled by the rotating blade, as well as the tower shadow effect, which gives the clearly marked notch after the tower passage at 0 deg azimuth. Different estimations of the deterministic contribution would result from different choices in the definition: for instance, adopting a shorter averaging time window to identify the deterministic variation would classify as deterministic contribution also the effects of large scale turbulence, thus returning an higher contribution.

Deterministic and stochastic contributions to the load variation are estimated at different mean wind speeds for the blade root flapwise and edgewise bending moments. From the original load time series, 'stochastic-only' time series are obtained by subtracting for each blade azimuthal position the corresponding deterministic load variation. The stochastic-only load time series would correspond to an ideal smart-rotor, with a cyclic control able to compensate for the whole deterministic load variation. The processed time series will be considered in the following sections in order to evaluate the fatigue contribution from the stochastic components of the loads.

The load variation in the blade root flapwise bending moment increases with the mean wind speed (red lines in figure 2). The main contribution originates from stochastic load variations (blue lines); nevertheless, deterministic variations are also relevant (black lines), and increase at higher wind speed, which is partly due to gravity contributions as the blade is pitched out of the rotor plane. In case of yaw misalignment, the increase in the overall load variation is mainly due to the deterministic component; a similar effect is also expected in case of partial wake operation.

The load variations at different mean wind speed provide a convenient term of comparison to estimate the load variation capability required to smart-rotor actuators. Furthermore, the load

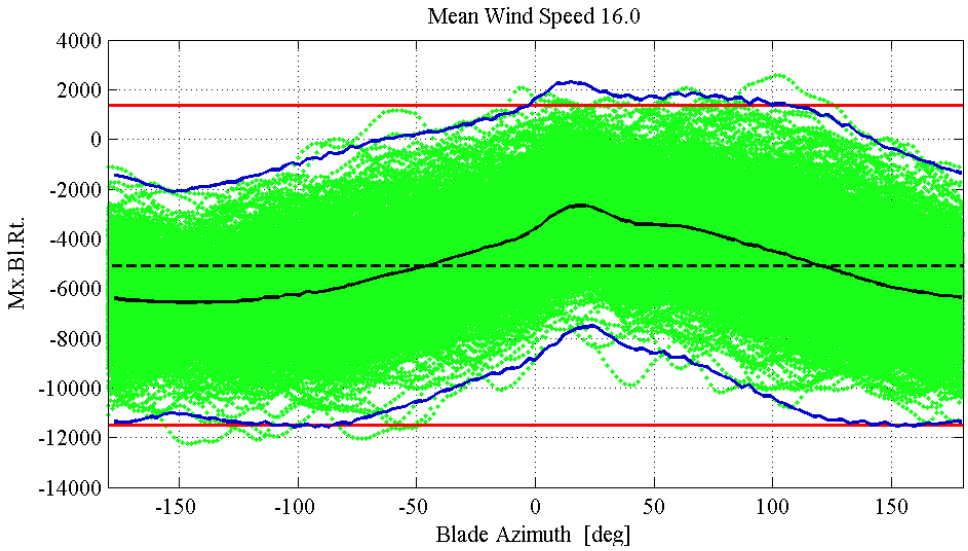

Figure 1. Blade root flapwise bending moment variations versus blade azimuthal position. Simulated time series (green dots), total variation of the simulated loads (red lines), deterministic contribution (black), stochastic contribution (blue).

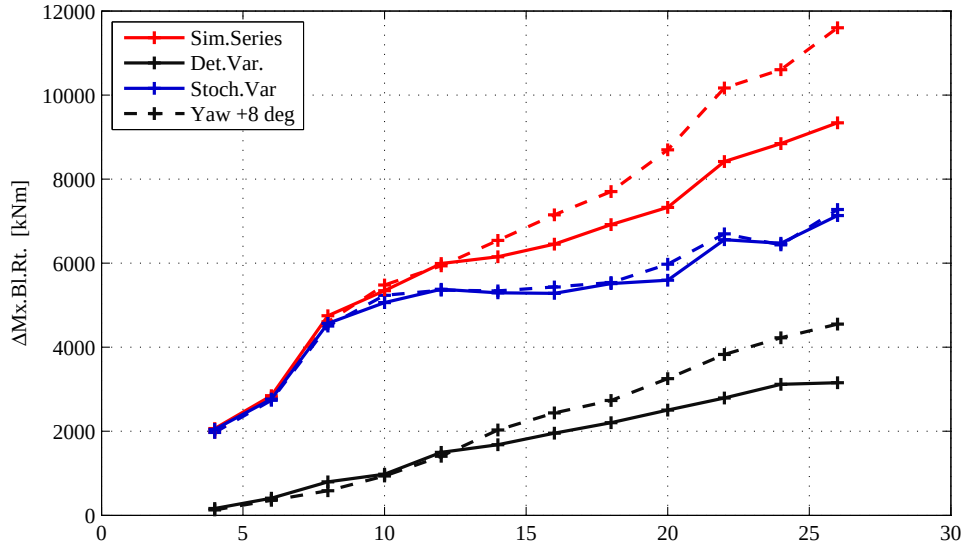

Figure 2. Blade root flapwise bending moment variations as function of mean wind speed. Simulated loads (red lines), deterministic load variation (black), stochastic load variation (blue). A case with yaw misalignment is given for comparison, dashed lines.

variation due to the deterministic component gives an estimate of the gain in load alleviation performances that could be achieved by including measured periodic disturbances in the smart-rotor controller, see for instance van Wingerden et al. [11].

3. Rain-flow counting fatigue analysis

The fatigue Damage Equivalent Loads (DEL) are computed from the load time series by applying a rain-flow counting (RFC) algorithm, and Palmgren-Miner rule for linear fatigue damage accumulation [12]. The life-time fatigue DEL accounts for the amount of time the turbine

is expected to operate at each wind speed condition; the wind distribution follows a Rayleigh distribution with average speed of 8.5 m/s, as prescribed by the IEC standard for a class II turbine [10].

Figure 3 shows the fatigue DEL for the blade root flapwise bending moment at different operating wind speed, and accounts for the amount of hours each wind speed is encountered during the turbine life-time. High wind speeds are less frequent than the low ones, nevertheless, operation at high wind still causes the largest contribution to the life-time fatigue damage. The fatigue DEL computed with a lower material exponent ($m = 8$ instead of 10) shows nearly no change below rated speed, while at high wind speeds, the DEL is lower than computed with the exponent 10, thus indicating larger fatigue contributions from wide range load cycles.

The same RFC analysis is performed on the time series obtained by subtracting the deterministic load variations (blue line with diamonds in figure 3). The fatigue DEL is lower, especially at wind speeds above rated; the overall life-time DEL is 11% lower than the lifetime fatigue load returned by the original time series. The fatigue reduction gives an estimate of the upper-limit to the fatigue load alleviation achievable by a smart-rotor control that only addresses cyclic load variations [13], and, at the same time, quantifies the importance of including periodic disturbance rejection in a smart-rotor control system.

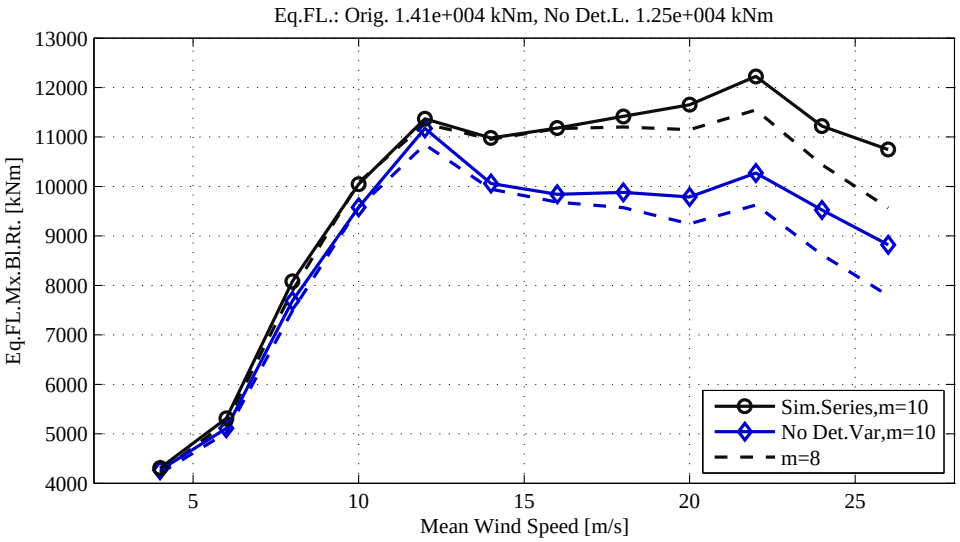

Figure 3. Blade root flapwise moment, fatigue damage equivalent loads (DEL) for operation at different mean wind speeds (weighted by the wind distribution). Results for simulated loads (black line) and for series without deterministic load variations (blue lines).

A similar analysis is performed for the blade edgewise bending moment (figure 4). As the fatigue damage is mainly gravity driven, the figure shows higher contributions for the wind speed bins that occur more frequently; furthermore, since the gravity load variation is periodic, the edgewise equivalent fatigue load for the time series without deterministic variation is less than half the original one.

Fatigue DEL for the shaft tilting and yawing moments show higher contributions for wind speeds at, and above rated (figure 5). The tower bottom flange fore-aft lifetime fatigue damage is mainly affected by operation at, and below rated wind speed (figure 6); on the contrary, the side-to-side moment receives most of the fatigue contribution from wind speed above rated.

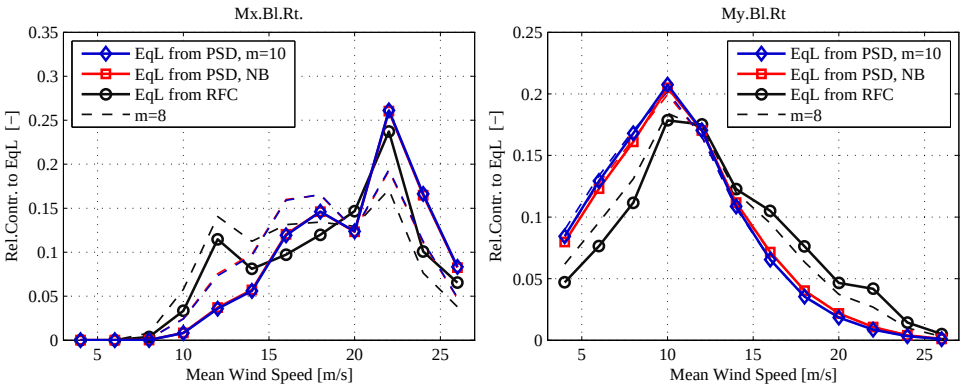

Figure 4. Blade root bending moments: flapwise (left), and edgewise (right). Relative contributions to the total lifetime fatigue DEL from operation at different mean wind speed, from rain-flow analysis (RFC) and spectral methods.

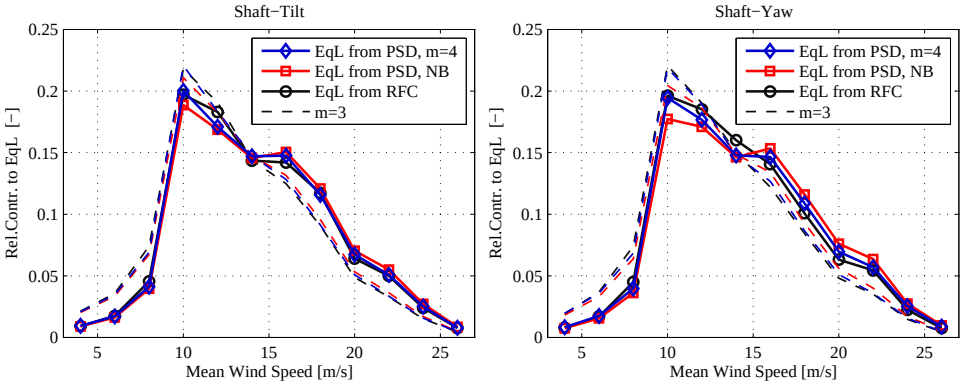

Figure 5. Shaft tilt (left) and yaw (right) moments, fatigue damage contributions from operation at different wind speed. Estimations from spectral and rain-flow counting methods.

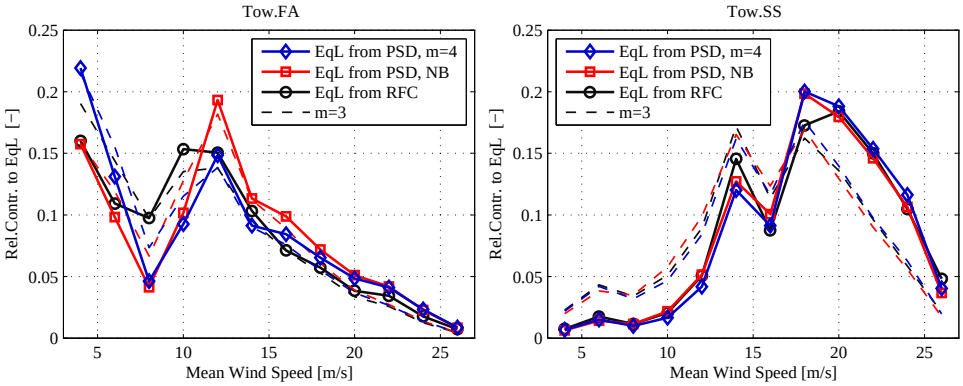

Figure 6. Tower bottom flange fore-aft (left) and side-to-side (right) bending moments, fatigue damage contributions from operation at different wind speed. Estimations from spectral and rain-flow counting methods.

4. Spectral load characterization: Power Spectral Density

The Power Spectral Density (PSD) of the load time series is computed using Welch's method as implemented in Matlab; the PSD obtained with different turbulence series for the same mean wind speed are then averaged together. A similar procedure is applied to the blade root moment time series where the deterministic variations of the load had been removed.

The blade root flapwise bending moment PSD (figure 7) is characterized by high energy content around the rotational frequency (1P = 0.2 Hz), and, less, at its first harmonic. The PSD rapidly decreases above 1-1.5 Hz, and its energy content is nearly insignificant above 2.5 Hz. The PSD of the series without deterministic loads variation shows, as expected, a marked reduction of the peak at the rotational frequency 1P (blue lines in figure 7); nevertheless, the peak at 1P still dominates the spectrum, thus implying that the stochastic component of the loads accumulates spectral energy contributions that, for a rotating blade, are mainly located around the rotational frequency.

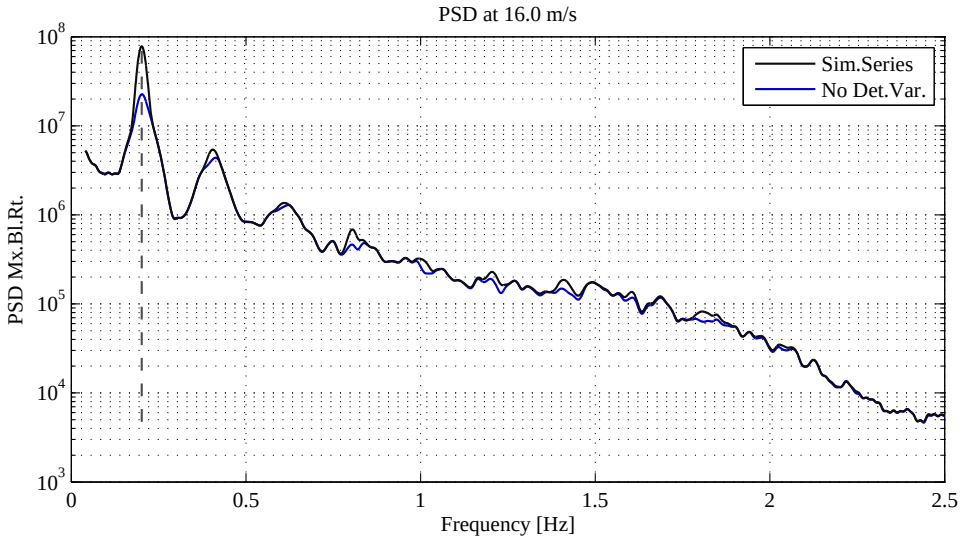

Figure 7. Blade root flapwise moment, Power Spectral Density (PSD) for the loads time series with mean wind speed of 16 m/s. Results for simulated loads (black line) and for series without deterministic load variations (blue lines).

5. Estimation of frequency contributions to fatigue damage

5.1. From PSD to fatigue damage ratio

Benasciutti and Tovo [14] propose a method to estimate the rain-flow fatigue damage from the stress power spectral density (PSD). The method is based on the assumption of Gaussian stationary process, and linear Palmgren-Miner rule for fatigue damage. The rain-flow fatigue damage ratio (D_{RFC}) is estimated as a weighted sum of the damage rate for a narrow-banded process (D_{NB}), and the range-mean counting damage (D_{RC}) [14]:

$$D_{RFC} = b_{wgt} D_{NB} + (1 - b_{wgt}) D_{RC}. \tag{1}$$

The range-mean counting damage is approximated as a function of the narrow-band damage rate (D_{NB}), the second bandwidth parameter α_2, and the fatigue strength exponent m:

$$D_{RFC} \approx b_{wgt} D_{NB} + (1 - b_{wgt}) D_{NB} \alpha_2^{m-1} = \left(b_{wgt} + (1 - b_{wgt}) \alpha_2^{m-1} \right) D_{NB}. \tag{2}$$

The expression for the narrow-band damage reads

$$D_{NB} = \frac{1}{S_0^m} \nu_0 \left(\sqrt{2\lambda_0} \right)^m \Gamma \left(1 + 0.5 \ m \right), \tag{3}$$

where S_0^m is the critical stress level, ν_0 is the rate of mean upcrossings, λ_i is the i-th spectral moment of the one-sided spectrum $W(\omega)$, and α_1 and α_2 are bandwidth parameters, as in [14]. The factor b_{wgt} in eq. (1) determines the weight between the narrow-banded fatigue damage and the range-mean counting damage; Benasciutti and Tovo [14] suggest an expression derived from empirical data fitting for the weight value, function of the first and second bandwidth parameters α:

$$b_{wgt} = \frac{(\alpha_1 - \alpha_2) \left[1.112 \left(1 + \alpha_1 \alpha_2 - \alpha_1 - \alpha_2 \right) e^{2.11 \ \alpha_2} + \alpha_1 - \alpha_2 \right]}{\left(\alpha_2 - 1 \right)^2}. \tag{4}$$

The method proposed by Benasciutti and Tovo is applied to the spectra of the bending moments computed in the previous section. The equivalent fatigue damage rates obtained at each mean wind speed are weighted by the wind distribution function, to obtain an indication of the relative contribution that operations at different mean speeds yield to the total life-time fatigue damage. The relative contributions obtained from the PSD method are compared to results from the rain-flow counting analysis (figures 4 – 6); the relative contributions returned under the narrow-banded process assumption (i.e. $b_{wgt} = 1$) are also plotted (red lines with squares).

In spite of fundamental differences between the two methods, the relative contributions computed by the frequency-domain PSD method are in good agreement with the figures from the time-domain RFC method. The strongest contributions to fatigue on the blade flapwise moment originate at high winds (figure 4, left), whereas the blade edgewise (figure 4, right), and the shaft bending moments (figure 5), show higher contributions from wind speeds around rated, which are more frequent. The narrow-banded (NB) approximation returns estimations very close to the full model ones for the blade and shaft bending moments, while larger differences are observed on the tower relative contributions (figure 6).

5.2. From PSD fatigue damage to frequency band contributions

The contribution to the total fatigue damage from a single frequency band $\mathrm{d}f_j$ is estimated by comparing the fatigue DEL computed on the full PSD, with the damage resulting from a spectrum where the energy content at the frequency band $\mathrm{d}f_j$ is set to zero. By repeating the same procedure for different frequency bins throughout the spectrum, is possible to characterize the frequency range of the loads that are responsible for the largest fatigue contributions.

To assess the validity of the spectral fatigue method, the results are compared with frequency contribution estimations based on RFC analysis of filtered time series. The series are filtered with a Butterworth low pass filter, and the RFC equivalent fatigue loads are computed for increasing cutoff frequency $f_{c,\mathrm{LPF}}$ (figure 8(a), top); as the cutoff frequency is raised, the fatigue loads converge to the ones of the original unfiltered time series.

The gradient of the curve gives an indication of the contribution brought to the total fatigue damage by loads in the specific frequency range (figure 8(a), bottom), and provides a term of comparison for the frequency fatigue contribution computed with the spectral method, figure 8(b) top. The agreement between the two methods is rather good; in both cases the highest fatigue contributions are characterized by loads with frequencies close to 1P, whereas very low fatigue contributions are reported for frequencies above 2 Hz. In the series where the deterministic variations of the loads have been removed (lighter colored lines), the contribution from frequencies around 1P is lower, but still remains the dominant one in the spectrum. A good

agreement between the RFC results and the ones based on spectral analysis is also reported for the edgewise, the shaft, and the tower bottom bending moments.

5.3. Fatigue damage spectrograms

Frequency contributions to the life-time fatigue DEL are organized in 'spectrogram-like' plots, where the load frequency is on the abscissa, and the mean wind speed on the ordinate. The surface color gives a qualitative indication of the contribution to the overall fatigue damage: dark red colors indicate 'harmful' loads, heavily contributing to the fatigue damage; blue colors indicate 'harmless' loads. The dashed white lines highlight the 1P and 3P rotational frequencies.

Fatigue on the blade root flapwise bending moment (figure 8(b)) is characterized by strong damage contributions from operations at high wind speed, and from loads with frequencies close to 1P; loads with frequencies above 2 Hz are found to be nearly 'harmless'.

The shaft fatigue damage (figure 9(a)) shows marked contributions close to 3P, and at the lower frequency range; the highest contributions to the life-time fatigue damage are reported from wind speed close to the rated one.

The spectrogram for the tower bottom fore-aft bending moment (figure 9(b)) also displays clear fatigue contributions from loads with frequency of 3P; in addition, the contribution of frequencies close to the first tower mode (0.3 Hz) are also well marked. It is worth noticing the considerable fatigue damage contribution at low wind speeds, where the 3P rotational frequency approaches the tower natural frequency.

6. Conclusion

The paper presents an analysis of the aeroelastic loads acting on a wind turbine during normal operation, and highlights the characteristics of the loads that are responsible for the strongest contributions to the fatigue damage.

The fatigue damage caused by deterministic load variations is estimated to be 11% of the total life-time damage, for the specific turbine model. The figure indicates the potential benefit of including deterministic (periodic) disturbance rejection in a smart-rotor control system. At the same time, it fixes an upper limit to the load alleviation achieved by purely cyclic control actions; information on the stochastic variations of the loads have to be included in the control algorithm to overcome this threshold.

The contribution to the blade root flapwise life-time fatigue damage from wind speeds above rated was found significantly higher than below rated conditions. It should be thus consider to exploit the control potentiality of a smart-rotor for different objectives below rated power, as, for instance, to increase the energy capture [15].

A method to characterize the load frequencies that cause the highest fatigue contributions is proposed, and proved consistent with rain-flow counting fatigue analysis. The results show that the loads inflicting the strongest fatigue damage on the blades are characterized by frequencies close to the rotational one, both in the case of deterministic, and stochastic load components. Accordingly, fatigue loads on fixed frames, as the shaft bearings or the tower bottom flange, show marked contributions from the 3P frequency; the fatigue damage on the tower receives important contributions also from loads with frequencies close to the structural one. In all cases, only minor contributions are received from loads with frequencies above 2 Hz, thus giving an indication on the bandwidth requirements for the active load alleviation system.

The paper identifies the loads that most heavily contribute to the structure fatigue damage. Active alleviation of these loads would return a direct benefit on the overall design requirements; the loads characteristics highlighted by the study can therefore provide useful indications for the future design of a smart-rotor with active load alleviation.

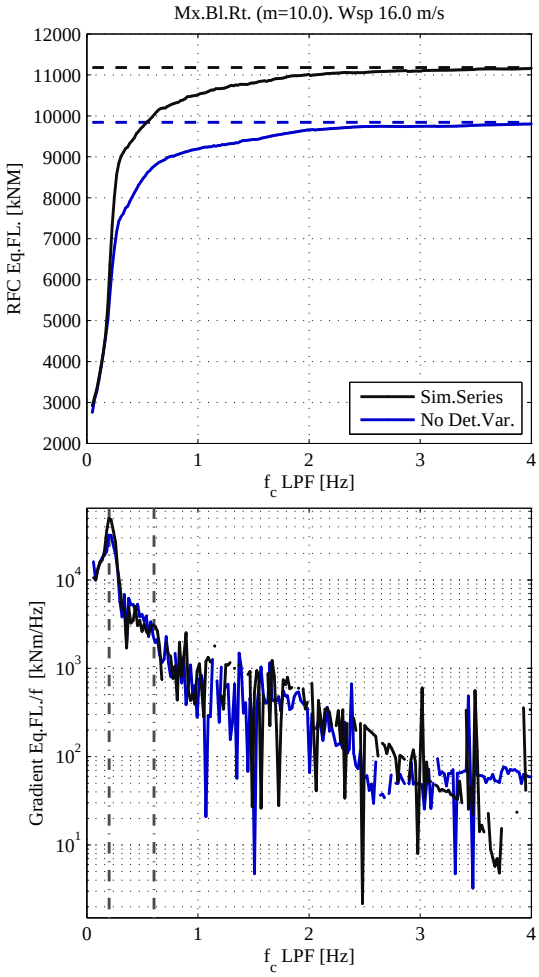

(a) Estimation from RFC on filtered time series

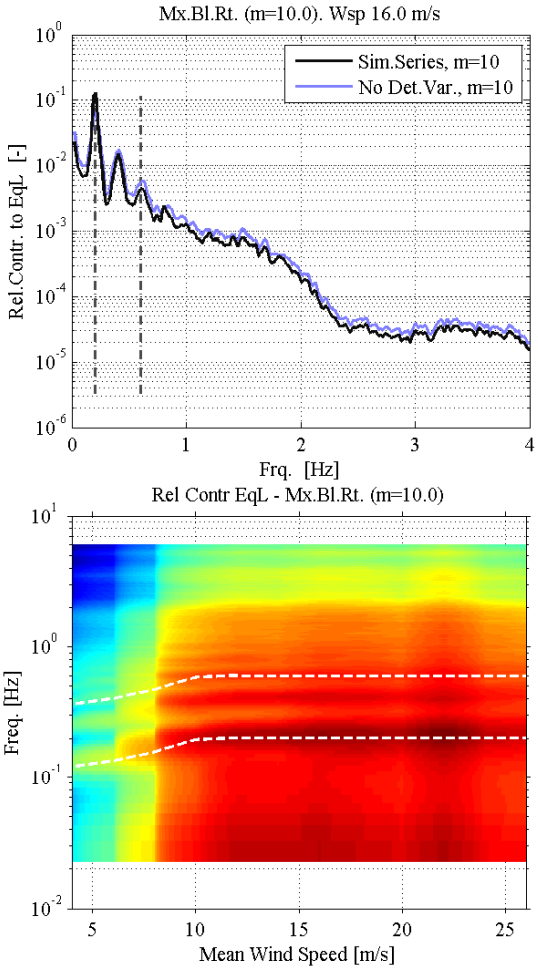

(b) Estimation from spectral methods

Figure 8. Blade root flapwise moment, frequency contribution to the total fatigue damage.

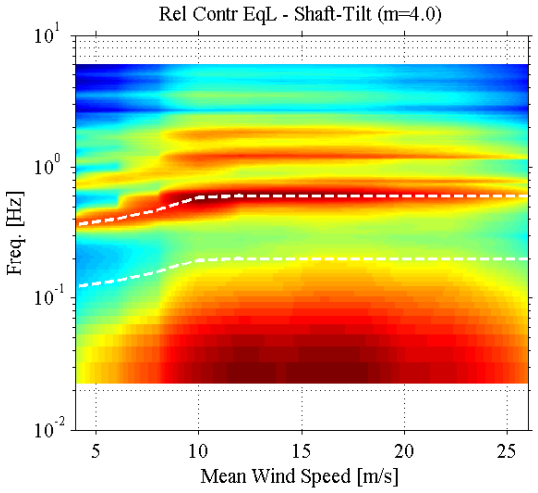

(a) Shaft tilt moment

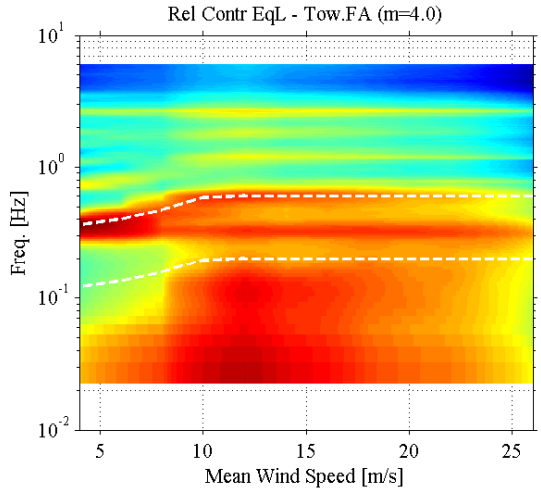

(b) Tower bottom fore-aft moment

Figure 9. Spectrograms of the estimation of the frequency fatigue contribution.

References

[1] Bossanyi E A 2003 *Wind Energy* **6** 119–128 ISSN 10954244

[2] Larsen T J, Madsen H A and Thomsen K 2005 *Wind Energy* **8** 67–80 ISSN 10954244

[3] Johnson S J, Baker J P, van Dam C P and Berg D 2010 *Wind Energy* **13** 239–253 ISSN 10954244

[4] Andersen P B, Henriksen L, Gaunaa M, Bak C and Buhl T 2010 *Wind Energy* **13** 193–206 ISSN 10954244

[5] Barlas T 2011 *Active aerodynamic load control on wind turbines: Aeroservoelastic modeling and wind tunnel* Ph.D. thesis TU Delft: Aerospace Engineering: Wind Energy Delft, Netherlands

[6] Jonkman J, Butterfield S, Musial W and Scott G 2009 Definition of a 5-MW reference wind turbine for offshore system development Tech. Rep. NREL/TP-500-38060 National Renewable Energy Laboratory (NREL)

[7] Larsen T J 2009 How 2 HAWC2 the user's manual Tech. Rep. R-1597(EN) Risoe National Laboratory. Technical University of Denmark

[8] Bergami L, Gaunaa M and Heinz J 2013 *Wind Energy* **16** 681–693 ISSN 1099-1824

[9] Hansen M H, Gaunaa M and Madsen H A 2004 A Beddoes-Leishman type dynamic stall model in state-space and indicial formulations Tech. Rep. R-1354(EN) Risoe National Laboratory, Roskilde (DK)

[10] International Electrotechnical Commission 2005 IEC 61400-1: Wind turbines part 1: Design requirements Tech. rep. International Electrotechnical Commission

[11] van Wingerden J W, Hulskamp A, Barlas T, Houtzager I, Bersee H, van Kuik G and Verhaegen M 2011 *IEEE Transactions on Control Systems Technology* **19** 284–296 ISSN 1063-6536

[12] Hansen M 2000 *Aerodynamics of wind turbines : rotors, loads and structure* (London: James & James) ISBN 9781902916064

[13] Houtzager I, van Wingerden J W and Verhaegen M 2012 *Wind Energy* ISSN 1099-1824

[14] Benasciutti D and Tovo R 2006 *Probabilistic Engineering Mechanics* **21** 287–299 ISSN 02668920

[15] Bergami L 2013 *Adaptive Trailing Edge Flaps for Active Load Alleviation in a Smart Rotor Configuration* Ph.D. thesis, DTU wind energy PhD-0020(EN) Technical University of Denmark Risoe Campus, Roskilde, Denmark